

# Optimal lithium targets for laser-plasma lithography

A.A. Andreev<sup>a,b</sup>, T. Ueda<sup>a</sup>, J. Limpouch<sup>c</sup>

<sup>a</sup>Yokogawa Electric Corporation, Tokyo, 180-8750 Japan

<sup>b</sup>Institute for Laser Physics, St. Petersburg 193232, Russia

<sup>c</sup>Czech Technical University, FNSPE, Břehová 7, 115 19 Prague, Czech Republic

## ABSTRACT

Lithium containing droplet and cluster targets irradiated by laser pulses are proposed as prospective source of for soft x-ray lithography. Analytical model and simulations show that laser with repetition rate of several MHz with energy of several mJ and pulse duration 10 ps is required.

**Keywords:** soft x-ray source, laser-produced plasmas, debris reduction

## 1. INTRODUCTION

There are three possible types of target for the reduction of debris: a fluid target in vacuum as a thick layer or spherical droplet [1]; a cluster gas puff target [2] and glass doped by metal [3]. In the first and second cases, the dense material absorbs laser radiation, is heated without debris, is converted into plasma, and the necessary wavelength radiation is emitted. In the last case, doped metal particles are heated by laser radiation due to the poor thermo-conductivity of glass material; the small ablation volume also reduces the deposition of particulates, and there is almost no debris in this case too.

It is well known [4] that the maximum reflection coefficient for an Si/Mo mirror is located in the interval with a maximum near 13.4 nm. For our purpose, we need line emission in the spectral range determined by reflectivity from the EUV mirror, for which the best candidates are Li, O, N and F (for example, see [5,6]).

For the rough estimation of resonant line emission we can use a simple formula:

$$J_{21} = 1.6 \cdot 10^{-19} E_{21} A_{21} N_2 \quad [\text{W}/\text{cm}^3],$$

where  $A_{21} = 0.7 \cdot 10^9 Z_{\text{nu}}^4 [\text{s}^{-1}]$  is the probability of 2 – 1 transition;  $E_{21} [\text{eV}]$  is the energy of transition; and  $N_2$  is the density of population number of level 2. For example, for an Li liquid target  $N_2 \leq 10^{22} \text{ cm}^{-3}$ , so  $\max J_{21} \leq 10^{15} \text{ W}/\text{cm}^3$ . As we want to produce the Ly- $\alpha$  line, the temperature of the plasma  $T_e$  should be not far from 100 eV, so velocity of sound  $c_s$  is near  $10^7 \text{ cm}/\text{s}$  and laser intensity  $I_L$  should be not less than  $10^{12} \text{ W}/\text{cm}^2$ . For a laser pulse duration  $t_L \approx 10 \text{ ps}$ , the created plasma length  $l_{pl} \approx 1 \mu\text{m}$  and for a laser focal spot area of  $10^{-4} \text{ cm}^2$  we obtain the EUV energy per laser pulse  $E_x \leq 0.01 \text{ mJ}$  and conversion efficiency  $K_x = E_L/E_x \leq 10^{-2}$ . For industrial lithography applications, we need power of approximately  $P_x = 10 \text{ W}$  EUV, so we need a repetition rate of laser  $R_r = P_x/E_x \geq 100 \text{ Hz}$  and total laser power  $\geq 100 \text{ W}$ . These are reasonable parameters of laser facilities in practice, so we will consider this situation in more detail.

Recently, line emission was obtained from two types of experiment with Li, one using capillary discharge [5] and the other a solid target [6]. The results of the experiment [5] showed spectral emission over the bandwidth of the X-ray grating. In addition to emission lines from doubly ionized lithium, lines were identified from five-times-ionized oxygen, because the used target adsorbed water vapor during its construction. The effective conversion efficiency from energy deposited in LiH to 13.5 nm radiation was 0.1% but there were certain problems with multi-time use of this source. For equivalent input energy, a pure lithium plasma is more efficient than a pure oxygen plasma, especially within the desired wavelength range of 13-14 nm. The H-like lithium spectrum is a narrow band ( $<0.1 \text{ nm}$ ) over the bandwidth of Si/Mo multi-layer mirrors. In contrast, most laser plasma sources being considered for EUV lithography use high Z targets [7-9], and hence their emission is broadband. The emission outside the bandwidth of the mirrors not only is wasted but also it is detrimental to the first collecting mirror in a lithography system because it is absorbed by the multi-layer coatings, resulting in unwanted heating. In contrast, the lithium plasma source would cause almost no off-band heating.

A lithium solid target was recently shown [6] to be a highly efficient line radiator at 13.5 nm (efficiency is near  $6 \cdot 10^{-4}$  for Li,  $2 \cdot 10^{-4}$  for F and  $6 \cdot 10^{-5}$  for O), but it is not a practical source for EUV lithography because of significant debris problems.

Pure Li is a rather expensive material but the solution of LiF salt in water is much cheaper. For these reasons we will consider in this paper LiF/LiCl:H<sub>2</sub>O, a droplet/cluster target, for maximum EUV emission because all the necessary elements are contained in this solution. We also propose to use laser pre-pulse to enhance the laser energy conversion into emission at the desired wavelength.

## 2. PRODUCTION OF DROPLETS AND CLUSTERS

Recent particle generators enable the production of droplets of size near 1 μm from a liquid with a concentration of more than  $n_d = 10^{10}$  particles/cm<sup>3</sup> and power of more than  $10^{10}$  particles per second [10]. The salt LiF dissolved in water produces an Li concentration of near 30% in the water droplet, which can be increased by drying the droplet.

When solution vapor flows into vacuum it can be supersaturated and solid density clusters will form. These clusters, which are held together by van der Waals force, can become quite large. We can estimate the size of cluster that will be desirable for illumination by a short pulse laser, if we require the time for cluster disassembling to be comparable to that of the laser pulse. We can estimate the time of this expansion if we assume sonic expansion and require the density to drop from the solid cluster density  $n_0$  to the surrounding ambient gas density  $n_s$ . The resulting cluster expansion time is approximately:

$$t_{ex} = (r_0/c_s)(n_0/n_s)^{1/3},$$

where  $r_0$  is the initial radius of the cluster. If the initial cluster is larger than about 30 nm in diameter, this corresponds to about  $10^5$  atoms per cluster and the surrounding bulk plasma has a density of  $n_e = 10^{14}$  cm<sup>-3</sup>, so pulses longer than 10 ps will interact with a cluster over a section of pulse. When clusters are present in the gas, collisional processes such as inverse bremsstrahlung and collisional ionization will dominate due to much higher density within the cluster.

## 3. DROPLET/CLUSTER PLASMA ABSORPTION

Even for the absorption coefficient of laser pulse as low as  $A_p \approx 0.01$ , the rate of ionization energy to absorbed laser energy  $E_i/E_{abs} \approx 0.25$  is rather small, and thus one can neglect the part of energy going to ionization of small solid/liquid particles (SSP) in the production of high density plasma particles (PP). The plasma skin layer length is  $l_{sn} \approx c/\omega_p \approx 10^{-5}$  cm and for SSP with a diameter of less than  $l_{sn}$ , the laser field penetrates PP totally.

In the analytical model of laser pulse interaction with a small sphere of dense plasma, we use the following assumptions: the initial plasma temperature is taken from the evaporation model [10]  $T = \text{const}(r)$  inside PP because the time of electron thermal wave propagation is small compared to other characteristic time scales; the Debye radius is small compared to other characteristic lengths; the initial density is determined by the vapor density in our model, and the density inside PP is homogeneous during laser heating and droplet expansion.

During laser-droplet interaction, the electron concentration in the evaporated material rises rapidly and at a certain time the plasma frequency can reach and even exceed the laser frequency at some distance from the particle center. In this case we should use a local absorption coefficient of the form:

$$K_p = k \frac{v}{\omega} \frac{\eta}{\left(\frac{\eta-3}{3}\right)^2 + \left(\frac{v}{\omega}\right)^2}, \quad (1)$$

where  $v = \max(v_{ei}, v_{en})$ ;  $v_{ei} = \sqrt{2\pi} Z^2 e^4 n_i / (m_e^{1/2} T_e^{3/2})$  and  $v_{en} \approx \sqrt{2\pi} Z^2 e^4 n_n / (m_e^{1/2} T_a^{3/2})$  are electron-ion and electron-atom collision frequencies;  $\eta = n_e/n_c$ , and  $n_c$  is critical density. From Eq. (1), at  $\eta = 3$  there is a resonant point and the absorption coefficient increases greatly at  $v/\omega < 1$ . The maximum absorption is  $A_{p, \max} \approx 3kr/(v/\omega)$ . The dynamics a small plasma sphere of volume  $V$  irradiated by laser radiation of intensity  $I_L$  is given by the next set of equations:

$$\begin{aligned} T_e N_e \frac{3}{r} \frac{\partial r}{\partial t} &= -\frac{3}{2} N_e \frac{\partial T_e}{\partial t} + VK_p I_L; & V &= \frac{4}{3} \pi r^3 \\ \frac{\partial^2 r}{\partial t^2} &= \frac{3P_e}{n_i m_i} \frac{1}{r} = \frac{3ZT_e}{m_i r}; & n_e &= Zn_i = Z \frac{N_i}{V} = Zn_{i0} \left(\frac{r_0}{r}\right)^3; & Z &\approx \frac{2}{3} (AT_e)^{1/3} \end{aligned} \quad (2)$$

We calculate this system roughly by supposing  $r \approx r_0 + c_s t$ , where  $c_s = (3ZT_e/m_i)^{1/2}$  and  $v \approx 0.4 \cdot 10^{-4} Z n_e T_e^{3/2}$ , and hence obtain temperature:

$$T_e \approx 0.3 \frac{I}{N_e} \left(\frac{r}{r_0}\right)^3 k r_0 \frac{v}{\omega} \frac{\eta}{\left(\frac{\eta-3}{3}\right)^2 + \left(\frac{v}{\omega}\right)^2} I_L \pi r_0^2 t \quad (3)$$

where  $T_e$  has maximum due to the maximum absorption efficiency, at the moment:

$$t_r \approx \frac{r_0}{c_{s0}} \left[ \left(\frac{Z n_{i0}}{3 n_c}\right)^{1/3} - 1 \right]$$

So laser pulse  $t_L$  should be close to this time for optimal interaction and  $t_L \approx 10$  ps is a very reasonable pulse duration for an interaction with a large cluster/droplet.

#### 4. DROPLET/CLUSTER PLASMA EMISSION

In the analytical model of plasma emission we suppose that the parameters of a plasma corona formed by the laser pulse do not change in space, but only in time. Continuum plasma emission from such a small particle as a droplet or cluster is very small in the interesting spectral range so we will neglect this radiation compared to the line emission.

The optimal conditions for the production of the maximum number of H-like ions correspond to an increase of laser intensity and temperature although the plasma temperature is limited by the requirement of sufficiently ionized but not over-ionized plasma. Another condition for optimal x-ray line emission from a bulk target is that X-ray line absorption length  $l_{x-abs}$  exceeds the extension of hot plasma  $l_{plasma}$  (i.e. that part of the plasma where a large fraction of H-like ions is present), namely  $l_{x-abs} > l_{plasma}$ . For our conditions, as we have high density plasma, the main cross section of absorption in the line center can be estimated as collisional:

$$l_{x-abs} \approx 1500 Z^* a_B \frac{c}{v_T} ,$$

where  $a_B$  is Bohr radius. For example, the collision absorption length of the line  $l_{x-abs}$  is  $5 \cdot 10^{-4}$  cm at  $T_e = 100$  eV, the resonant absorption length is  $l_{res} = 1/\sigma_x n_a = 10^{-2}$  cm for gas concentration  $n_a = 10^{14} \text{ cm}^{-3}$ , where  $\sigma_x \approx \pi \lambda_x^2$  and  $\lambda_x \approx 13$  nm. So for the cluster target inside a gas flow, we can take  $n_{cluster} = 10^{18} \text{ cm}^{-3}$  and surrounding gas  $n_{gas} = 10^{14} \text{ cm}^{-3}$  with the length of gas flow near 100  $\mu\text{m}$  in vacuum.

In the analytical model, we assume that the parameters of the plasma corona formed by laser prepulse do not change in space during the main pulse. For these reasons, we consider the next set of equations: Plasma temperature is governed by Eq. (3) and the electron plasma density during plasma expansion depends on time, as follows

$$n_e \approx n_{e0} [r_0 / (c_s t + r_0)]^3 , \quad (4)$$

For a Li target in the initial stage, we suppose that there are only He-like ions, and ion density is determined by ionization and three-body recombination of the included ions. The symbol  $n_{He}$  denotes density of He-like ions,  $n_H$  is population of H-like ions,  $n_{nu}$  is population of fully stripped ions. The rate equations write, as follows

$$\begin{aligned} \partial n_{He} / \partial t &\approx -\gamma_i^{He} n_{He} \\ \partial n_H / \partial t &\approx \gamma_i^{He} n_{He} - \gamma_r^H n_H - \gamma_r^{He} n_H \\ \partial n_{nu} / \partial t &\approx \gamma_r^H n_H - \gamma_r^H n_{nu} , \end{aligned} \quad (5)$$

where the ionization rate of  $I$ -like ion is  $\gamma_i^I = n_e \langle \sigma v \rangle_I$ , and the Seaton's formula is used for cross section:  $\langle \sigma v \rangle_I = 4.3 \cdot 10^{-3} (Ry / J_I)^{3/2} (T_e / J_I) \exp(-J_I / T_e)$ . Symbol  $J_I$  is ionization potential of  $I$ -like ions; the recombination rate is  $\gamma_r^I = n_I 4 \cdot 10^{-27} Z_{nu}^3 T_e^{-9/2} n_e^2$  dominated by three-body recombination as electron density is high. The population density of the upper state ( $n=2$ ) of H-like ions is described by the following equation

$$\partial N_2/\partial t = -A_{21}N_2 - \langle \sigma v \rangle_{21} n_e N_2 + \langle \sigma v \rangle_{12} n_e n_H, \quad (6)$$

where  $\langle \sigma v \rangle_{mn} = 6.4 \cdot 10^{-8} f_{nm} (Ry/E_{mn})^{3/2} (E_{mn}/T_e)^{1/2} \exp(-E_{mn}/T_e)$ ;  $E_{mn}$  is energy of transition; and  $f_{nm} = (32/3\pi\sqrt{3})nm^3/(m^2 - n^2)$ . For initial population density, we assume that all ions are in the lower state.

The emitted energy density in the spectral line of  $2 \rightarrow 1$  transition in optically thin plasma is written, as follows

$$\partial W_{21}/\partial t = E_{21}A_{21}N_2. \quad (7)$$

From Eq. (2) we obtain:

$$T_e \approx K_p I_L/3n_e c_s \approx T_0 (I_L/I_0)^{1/4} (1 + t/t_L)^{-1/2}, \quad (8)$$

where,  $T_0 = 50$  eV and  $I_0 = 10^{12}$  W/cm<sup>2</sup>.

The population  $n_H$  of H-like ions is approximated using Eq. (5), as follows

$$n_H \approx (n_e/Z_{nu}) [1 - \exp(-\gamma_i^{He} t)] \exp(-\gamma_i^H t) \approx n_e^2 T_e^{1/2} \exp(-J_{He}/T_e)$$

This expression shows that the maximum concentration of H-like ions is at time  $t_m \approx (1/\gamma_i^{He}) \ln(\gamma_i^{He}/\gamma_i^H) \approx 1/\gamma_i^H$ . This time is less than 1 ps for our parameters and as we do not want to use a very short laser pulses, we put  $t = t_L$  and we search for the optimal conditions for line emission varying laser intensity.

We obtain the emitted energy density in the assumed line from Eqs. (6) and (7)

$$W_{21} \approx W_0 (T_e/J_H)^{3/2} \exp(-E_{21}/T_e - \gamma_i^H t_L)$$

where,  $\gamma_i^H \approx \gamma_0 (T_e/J_H)^{1/2} \exp(-J_H/T_e)$  and  $W_0 = 10$  J/cm<sup>3</sup>. Then the approximate formula is obtained for integrated fluency  $F_x$  in the Ly- $\alpha$  line

$$F_x = F_{21} \approx F_0 x^{3/2} \exp[-x(1 + b x^{1/2} \exp(-x))] , \quad (9)$$

where  $x = (I_{mL}/I_L)^{1/4}$ ,  $F_0 = 10$  J/cm<sup>2</sup>, and  $b = 0.3$ .

The developed analytical model shows that an optimum laser intensity for laser energy transformation into emission of lithium Ly- $\alpha$  line exists and is given by the following formula

$$I_{mL} \approx I_0 (E_{21}/E_0)^{7/9} (r_0/r_m)^{-2/3} (J_H/J_m)^{5/3} (t_L/t_0)^{4/3},$$

where  $E_0 = 0.1$  keV,  $r_m = 50$  nm,  $t_0 = 10$  ps, and  $J_m = 200$  eV.

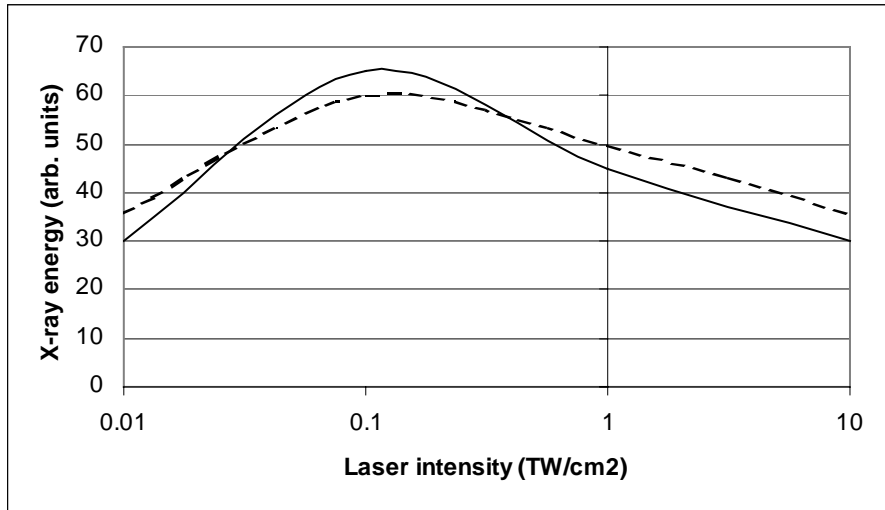


Fig. 1 Energy emitted in Li Ly- $\alpha$  line versus main pulse laser intensity for laser pulse length 10 ps, laser wavelength 800 nm and optimum pulse separation  $\Delta\tau$ . Solid line - experimental values [5], dashed line – our formula (9).

Figure 1 demonstrates a agreement of our formula (9) with the experimental values of Ref. [5].

## 5. RESULTS OF NUMERICAL SIMULATIONS

We use our hydrocode [11] to model the laser pulse interaction with the cluster/droplet target. The plasma dynamics are described by a one-fluid, two-temperature Lagrangian code with the electron and ion thermal conductivities and ion viscosity. The absorption coefficient of laser radiation by the plasma sphere takes into account the resonant conditions. Radiation transport in lines is modeled as a post-processor to the hydrocode [12]. The spectra of line emission are calculated together with a self-consistent description of the excitation kinetics. The cross sections for collision and collision-less transitions for all elements and all ionization and excitation states are taken into account in the model.

In order to model layer target, we assume normally incident laser pulse of duration  $t_L = 10$  ps and maximum intensity  $I_L = 10^{13}$  W/cm<sup>2</sup> on a Li plane foil of initial thickness  $l_i = 0.3$  μm and density  $\rho_i = 0.5$  g/cm<sup>3</sup>. The simulation results show very sharp density gradients and plasma corona not long enough to produce the necessary amount of EUV radiation despite suitable charge distribution. In order to increase plasma length, we propose to use a pre-pulse at time  $\Delta\tau$  ahead of the main laser pulse. Here, for simplicity, the delay of the main pulse is  $\Delta\tau = 189$  ps. The calculated plasma hydrodynamic parameters are shown at the figures below. Figures 2,3 show profiles of plasma density, electron temperature respectively. Average ion charge in the corona is between 2 and 3.

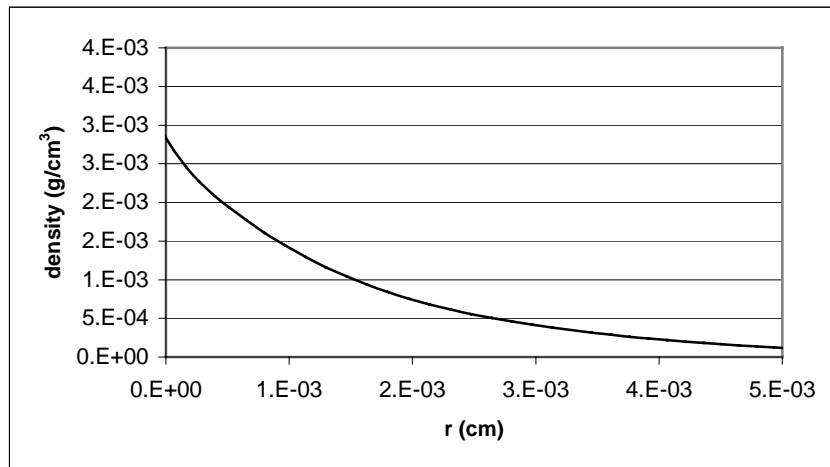


Fig.2 Plasma density profile in corona at the main pulse maximum of intensity  $10^{13}$  W/cm<sup>2</sup> incident with delay  $\Delta\tau=189$  ps after pre-pulse of intensity  $10^{12}$  W/cm<sup>2</sup>.

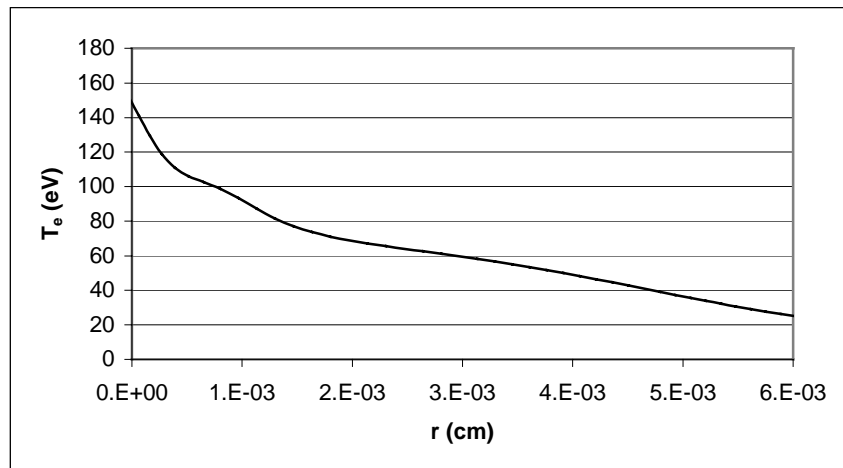


Fig.3 Electron temperature in plasma corona. The same conditions as in Fig.2.

These figures show that the plasma corona has suitable hydrodynamic parameters for emission of the required amount of EUV radiation. These plasma parameters are applied in calculation of EUV emission. The emitted spectral energy density (integrated over time up to  $3t_L$ ) is plotted in Fig.4. Here, Ly- $\alpha$  line emission is much intense than the other lines and satellites.

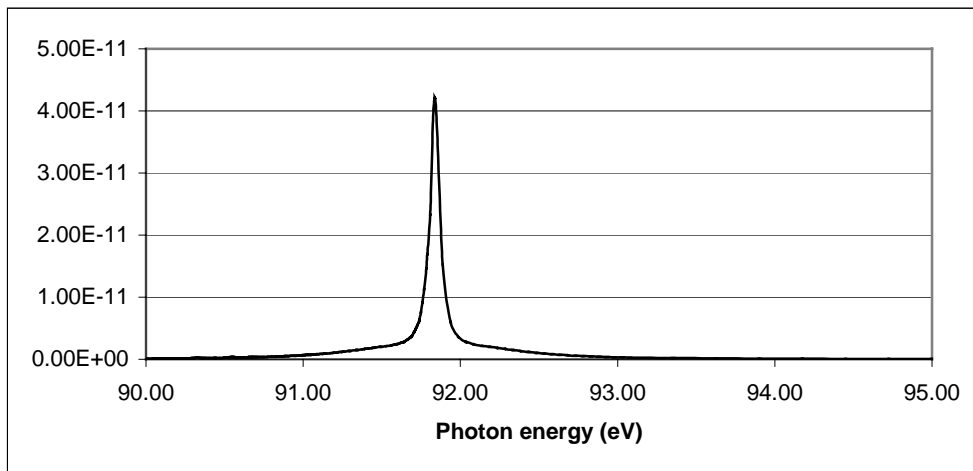


Fig. 4 Integral over time up to  $3t_L$  spectral energy density in vicinity of Li Ly- $\alpha$  line.

The energy density in Li Ly- $\alpha$  line emitted into the solid angle  $\Delta\Omega$  from Fig.4 is

$$\epsilon_x = (\Delta\Omega/2\pi) 3 \times 10^{-2} \text{ J/cm}^2.$$

We obtain  $E_x = 10^{-6}$  J for the laser spot size of  $170 \mu\text{m}$  and solid angle of emission  $\Delta\Omega = 0.2\pi$ . Thus, we require a laser with repetition rate 10 MHz of pulse energy  $E_L = 30$  mJ, pulse duration  $t_L = 10$  ps and intensity  $I_L = 10^{13}$  W/cm $^2$  to produce 10 W EUV radiation in the spectral range 0.2 eV at wavelength 13.5 nm from the layer target.

In order to analyze performance of the cluster target, we modeled solid spherical Li target of initial radius

$r_i = 0.05 \mu\text{m}$  and density  $\rho_i = 0.5 \text{ g/cm}^3$  irradiated by laser pulse of duration  $t_L = 10$  ps and of maximum intensity  $I_L = 10^{12}$  W/cm $^2$ . The simulations show hydrodynamics parameters of the plasma corona suitable for emission of the required amount of EUV radiation. The calculated plasma scale length about  $0.3 \mu\text{m}$ , average temperature of 30 eV and average density of  $0.001 \text{ g/cm}^3$  at the maximum of laser pulse are sufficient for effective Ly- $\alpha$  line emission. Then time integrated EUV emission, calculated by the FLY code [13], is plotted in Figure 5. The Ly- $\alpha$  line emission is dominant and practically all emission is in the best reflection region of Si/Mo mirrors.

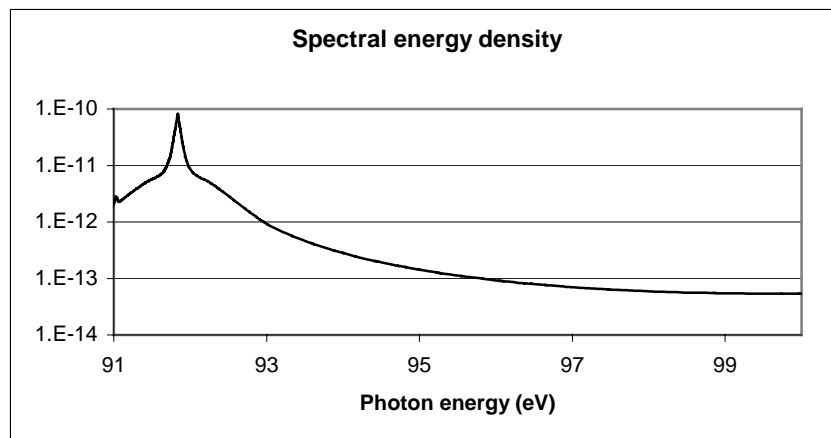


Fig. 5 Time integrated spectral energy density of plasma emission

Integrating this data, the fluence emitted into the angle  $\Delta\Omega$  from one cluster is found

$$\epsilon_{cl} = (\Delta\Omega/2\pi) 3 \times 10^{-3} \text{ J/cm}^2.$$

The total area of all clusters in the focal volume must be found in order to calculate the total emitted energy emitted. The area of all clusters is estimated, as follows:

$$S_{cl}^{tot} \approx S_f (S_{cl}/S_{pl}) (L_f/D_{pl}),$$

where,  $S_f$  is laser focal spot area;  $D_{pl}$  and  $S_{pl}$  are the diameter and area of the cluster plasma sphere;  $S_{cl}$  is area of cluster; and  $L_f$  is length of focal volume. For the laser spot size  $30 \mu\text{m}$ ,  $D_{pl} \approx 0.3 \mu\text{m}$ ,  $L_f \approx 4D_f$  and solid angle of emitted EUV radiation  $\Delta\Omega = 0.4\pi$ , the total emitted energy of  $E_x \approx 0.510^{-5} \text{ J}$  is obtained. From this value of emitted energy we can conclude that to get the necessary power of EUV radiation  $P_x = 10 \text{ W}$  in the spectral range  $0.2 \text{ eV}$  at wavelength  $13.5 \text{ nm}$  from the  $\text{Li:F:H}_2\text{O}$  droplet, our laser facility requires the repetition rate of  $2 \text{ MHz}$ , and hence the average power of the laser should be  $2 \text{ kW}$ .

In order to analyze the performance of a droplet target, we modeled the dynamics of liquid Li spherical target of initial radius  $r_t = 0.7 \mu\text{m}$  and of density  $\rho_t = 0.5 \text{ g/cm}^3$  irradiated by a laser pulse of duration  $t_L = 10 \text{ ps}$  and of maximum intensity  $I_L = 6.3 \times 10^{12} \text{ W/cm}^2$ . The simulation results show sharp density gradients and plasma length insufficient for production of the required amount of EUV radiation. Again, an application of laser pre-pulse is proposed in order to increase the plasma length. In this case, the assumed main pulse delay is  $\Delta\tau = 100 \text{ ps}$  and the prepulse intensity is  $I_{pL} = 6 \times 10^{11} \text{ W/cm}^2$ .

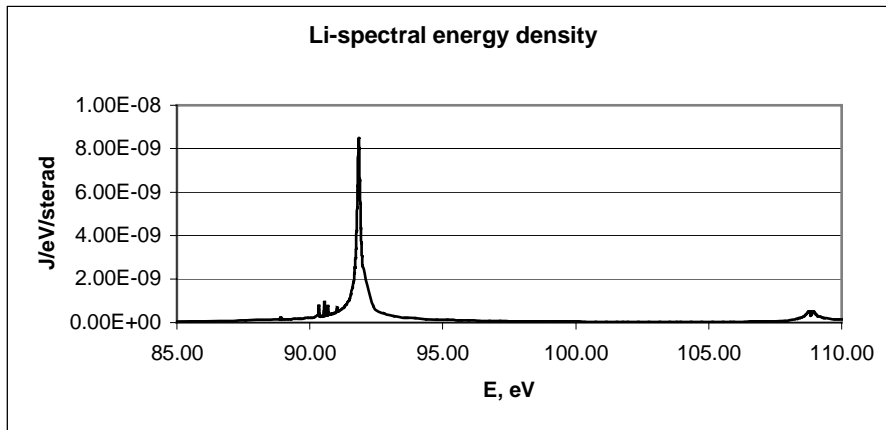


Fig. 6 Time integrated spectral energy density of emission from Li droplet.

The simulations show that the plasma corona has reasonable hydrodynamics parameters to produce the required amount of EUV radiation. We obtain the plasma scale length of  $10 \mu\text{m}$ , average temperature of  $20 \text{ eV}$  and average density of  $0.001 \text{ g/cm}^3$  at the moment  $30 \text{ ps}$  after the main pulse maximum. Approximately the same data are obtained when pure water target is considered. EUV emission is calculated and the results are shown in Figure 6. The Ly- $\alpha$  line emission is much more intense than the other lines and satellites and practically all emission is in the best reflection region of Si/Mo mirrors.

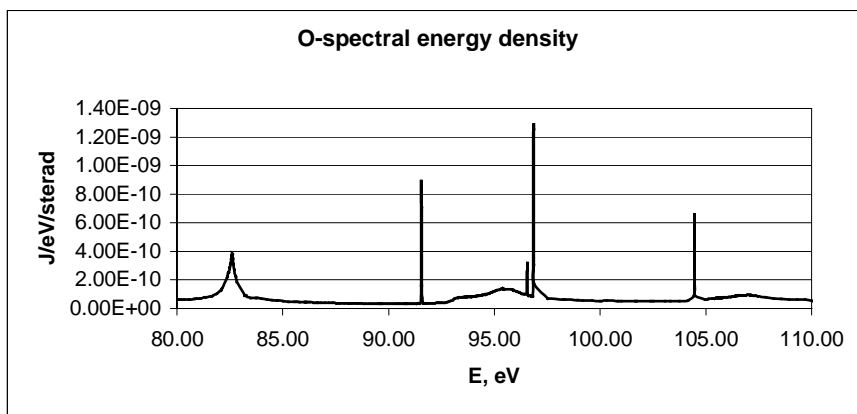


Fig.7 Time integrated spectral energy density of emission from water droplet.

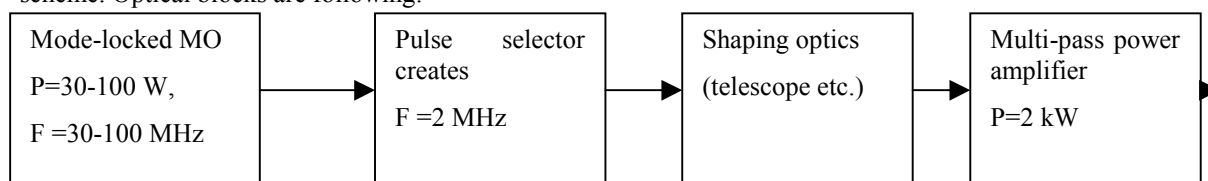
The code does not include Stark broadening of the lines of He-like oxygen. Thus their peak intensity is overestimated in Fig.7. The overall spectral intensity in the above interval is 30 times less than from Li target. The total number  $N_d^{\text{tot}}$  of all droplets in the focal spot can be estimated, as follows  $N_d^{\text{tot}} \approx n_d S_f L_f$ ,

where  $S_f$  is laser focal spot cross-section and  $L_f$  is focus length. We obtain the total emitted energy of  $E_x \approx 0.210^{-4}$  J for the laser spot size 100  $\mu\text{m}$ ,  $L_f \approx 4D_f$  and solid angle of EUV emission  $\Delta\Omega = 0.4\pi$ .

We can conclude that laser facility must have the repetition rate of 0.4 MHz in order to reach the required power  $P_x = 20$  W of EUV radiation in the spectral interval of 0.2 eV at wavelength 13.5 nm emitted from the Li:F:H<sub>2</sub>O droplets, and hence the average laser power should be near 0.4 kW.

In simulations, we have found a weak dependence of EUV emission on the laser pulse duration. The effect of increasing laser energy by increasing laser pulse duration on EUV energy is canceled out by the slow deposition rate and the shift of the optimum population, thus keeping emitted energy almost unchanged.

A method of construction the required laser facility was proposed in Ref. [14]. Such a laser can be built using the MOPA scheme. Optical blocks are following:



Because the output beam of this laser system should have high quality, some method for compensation of the strong thermo-optical distortions must be implemented. Among possible methods based on phase conjugation are: adaptive optics with deformable and/or segmented mirrors; four-wave mixing on liquid crystals (freeze phase conjugation)[15]; four-wave phase conjugation on thermal gratings in the loop schemes. Most simple and effective SBS phase conjugation could not be used because of large time relaxation of ultra-sound.

## 6. CONCLUSIONS

Analytical model and simulations show that prevailing part of droplet/cluster LiF water solvent emission is located in the efficient spectral region of Si/Mo x-ray optics. Laser with repetition rate of several MHz with energy of several mJ and pulse duration 10 ps is sufficient to produce necessary soft x-ray radiation power for x-ray lithography when an optimum target is used.

## ACKNOWLEDGEMENTS

This work was supported by the R&D IPE, the MS and Technology Center, and the New Energy and Industrial Technology Development Organization. The work of JL was supported by grant LN00A100 of Czech Ministry of Education.

## REFERENCES

1. M. Hertz et al., *Proc. SPIE* **3767**, p.2, 1999.
2. G. D. Kubiak et al., *Proc. SPIE* **3331**, p. 81, 1998.
3. H. Nakano et al., *Appl. Phys. Lett.* **70**, p.16, 1997.
4. W. Silfast et al., *J. Vac. Sci. Technol.* **B 10**, p.3126, 1992.
5. F. Jin. and M. Richardson., *Applied Optics* **34**, p.5750, 1995.
6. G. Schriever et al., *Appl. Optics.* **37**, p.1243, 1998.
7. P. Bogey et al., *J. Opt. Soc. Am.* **58**, p. 203,1968.
8. M. Klosner, H. Bender, W. Silfast, J. Rocca, *Optics Letters* **22**, p.34, 1997.
9. G.D. Kubiak et al., *Proc. SPIE* **3331**, p. 81, 1998.
10. A.A. Andreev, T. Ueda, M. Wakamatsu, *Int. Opt. Congress*, Skt.Petersburg, Russia, October 2000
11. A.A. Andreev, J. Limpouch, *J. Plasma Phys.* **62**, pp. 179 – 193, 1999.
12. A.A.Andreev , J. Limpouch, H. Nakano, *Proc. SPIE* **3934**, pp.52-60, 2000.
13. R.W. Lee, J.T. Larsen, *J.Q.S.R.T.* **56**, pp. 535-556, 1996.
14. V.E. Yashin, S.A. Chizhov et al., *Proc. SPIE* **3264**, p.43, 1998.
15. V.Berenberg et al., *Proc SPIE.* **4095**, pp.939-944, 2000.